Nano-Viewpoint in Modeling and Investigation of the D/M/D Transparent-Conductive Layer

Gholamhosain Haidari (moh1135@gmail.com)
Shahrekord University https://orcid.org/0000-0003-2400-9280

Research Article

Keywords: Transparent conductive film, Dielectric/metal/dielectric, FDTD design, Very thin metallic film, Plasmonic nanostructure

Posted Date: May 5th, 2021

DOI: https://doi.org/10.21203/rs.3.rs-453928/v1

Version of Record: A version of this preprint was published at Plasmonics on August 16th, 2021. See the published version at https://doi.org/10.1007/s11468-021-01523-5.

Abstract

A transparent-conductive film (TCF) is widely used in various electro-optical devices. The dielectric/metal/dielectric(D/M/D) as one type of TCF has been highly considered due to more advantages, such as the possibility of selecting different materials and engineering other properties. For pre-fabrication design, it is often modeled with a 1D photonic crystal. This model needs to be improved due to the low thickness of the metal layer. This thin metallic layer leads to a nanostructure instead of a uniform layer. In this study, after proper nanostructure modeling, the 3D-FDTD method was used to simulate different optical properties of the structure. The first aspect of the importance of the nanostructured model is to address the serious plasmonic resonant losses. They are associated with the complicated metallic form in D/M/D that is not considered in conventional modeling. The simulation results showed that for Ag, plasmonic loss peaks show a wide distribution over the visible. About Al, these peaks show a more significant distribution at the beginning of the visible spectrum. In both, plasmonic loss behavior tends to red-shift. About optical transition, Al does not offer a notable advantage over Ag. Due to the intense excitation of plasmonic losses when the metal layer has pores, a layer of entirely connected nanoparticles with the least possible thickness can have the desired properties. The increased rough surface of the dielectric layer due to the nanostructured metallic layer was also modeled.

1. Introduction

Transparent conductive films (TCF) are transparent and conductive thin layers. They are an essential component in various optoelectronic components such as liquid crystal displays, OLEDs, touch screens, and photovoltaics [1, 2]. For TCF, a metal oxide layer using indium tin oxide (ITO), fluorine-doped tin oxide (FTO), and doped zinc oxide is usually used [2]. Although these are widely used, alternative competitors are also introduced. Other conductive oxides with a broader transparent spectrum, dielectric/metal/dielectric multilayer structure instead of monolayer structure, conductive polymers, metal grid, and random metal grid. Carbon nanotubes, graphene, nanowire mesh, and ultra-thin metal films have also been proposed [1-4]. To date, one of the most practical TCFs is ITO. The sheet resistance and optical transition of ITO depend on its thickness and fabrication method [1, 5]. For an ITO layer at a thickness of 200 nm, specifications such as sheet resistance of the order $11 * 10^{-2}\ \Omega^{-1}$ and the optical transition of ~ 86% at 550 nm wavelength has been reported [6]. But the main problem with ITOs is that they are expensive (restricted source) and have limited mechanical flexibility [1]. Among the various other TCF options, the dielectric/metal/dielectric thin film (or D/M/D multilayer arrangements) has proven its worth [5, 6]. Moreover, various dielectrics using metal oxides (like MoO3, V2O5, ZnO, and WO3) and ZnS have been investigated as dielectric layers [1, 7, 8]. In general, to use D/M/Ds as transparent conductive electrodes, a load carrier density of 1020 cm-3 is required to achieve low resistance. Also, the bandgap of the structure should be larger than 3 eV to prevent light absorption. Such structures can also have excellent flexibility, high conductivity, and good transmission. They can also be placed on the substrates, usually at room temperature, by different chemical or physical methods [9, 10]. Also, the D/M/D work function can be controlled by the dielectric selection, allowing them to be used as a cathode-anode or

even as an intermediate electrode in tandem solar cells. To theoretical study and simulation, 3D modeling is the first step. In simple modeling, the only optical difference in depth is to be considered. After selecting the type of material, the theoretical optimization of this structure involves determining the thickness of these three layers. Hence, reflection and transmission can be calculated such as the Transfer Matrix Method (TMM) [11-13]. Moreover, the refractive index of the layers is typically assumed to be constant, but the dispersion of the refractive index can also be considered in this method. Determining the thickness of the metal layer is one of the significant design challenges of this structure. This thickness should be large enough to ensure the conductivity of the layer and at the same time, be as small as possible so as not to impede the required transparency. In D/M/D structures, Ag is usually chosen as the metal layer due to its high conductivity and reasonable price [14]. If the thickness of the metal layer (Ag) is less than ~8 nm, discontinuities will occur on its surface, which will increase the sheet resistance. Also, its thickness should not be more than 20 nm because it increases the reflection in the visible section. Depending on the nominal thickness at this very thin domain of metal, thin-film growth can occur in three ways Volmer-Webber (island growth), Frank-Van der Merwe (layer by layer growth), and Stranski-Krastanov (an intermediate case) [15]. The Volmer-Weber happens with low wettability materials forms isolated islands. This method is the typical growth accessible by soft metals (like Ag) onto insulators [16]. Hence, one of the design challenges of these D/M/D structures shows itself. In other words, at least the metal layer cannot have a homogeneous shape (uniform thin film). Therefore, the last optimized thickness, which is calculated based on the assumption of a uniform and homogeneous layer, seems to need more investigation. Certainly, if the righter morphology of the metal layer is considered, more details will be apparent in the D/M/D design. In contrast to TMM, there is a finite-difference time-domain (FDTD) simulation method that allows different 3D aspects of structure to be considered [17]. In a few studies for designing the D/M/D, the FDTD method has been used, but the assumption of uniform layers has remained. Therefore, those results can be achieved with TMM, too [18, 19].

In this study, first, the nanostructured D/M/D was modeled appropriately. Then, by selecting the typical materials, the near and far-field results were obtained by the FDTD method. The results obtained by 3D-FDTD modeling were analyzed and compared with TMM results. Moreover, the details that were not considered by the TMM method were highlighted and studied. Also, the change of metal material from Ag to Al and the effect of adding surface roughness to the nano-based modeling were investigated.

2. Modeling Method - Simulation

A. 1D photonic structure

In this study, the TiO2/Ag/In2O3 was chosen for considering the nano aspect with 3D FDTD simulation against the commonly TMM design. The Lumerical simulator is used for FDTD simulation. In selecting this typical D/M/D, both more flexible and less amount of In2O3 has been considered. Simultaneously, it has the advantage that the top layer is similar to ITO, that its various effects have been widely used in optoelectronic applications [20, 21]. Different aspects of introducing the simulation are given in Figure 1 (1-1 to 1-6). Firstly, an initial value for the thickness of the three layers was obtained based on the

approximation of a homogeneous and uniform layer with a sharp interface (1D photonic structure introduced in Figure 1.1). The following are the steps for calculating thicknesses based on this simple model: the subtitles a, b, and c in TiO2(**a** nm)/Ag(**b** nm)/In2O3(**c** nm) refer to layer thicknesses. At first, a and b were assumed to be equal to 25 nm and the total reflectance of the D/M/D was calculated at wavelength 550 nm for different thicknesses of Ag (Figure 2, curve M). According to this curve, for the next step, 10 nm was selected for the Ag layer. Then, the total reflectance was calculated for the chosen b=10 nm and c=25 nm as well as different values of a-parameter (Figure 2, curve N). In this section, the a=33 nm was chosen for TiO2. Finally, the total reflectance was calculated for a=33 nm and b=10 nm and different values of c-parameter. In this section, the c=33 nm was selected for In2O3 (Figure 2, curve O). Finally, the D/M/D becomes the TiO2(33 nm)/Ag(10 nm)/In2O3(33 nm). Figure 3 shows the reflection, absorption, and transition spectrum of the last D/M/D design. In Figure 3, there is a good match between TMM and FDTD method, too. The mesh size of the FDTD method was 2 nm for the D/M/D structure.

B. Nanostructure viewpoint

As mentioned in the introduction and thin films grow epitaxially at an interface, the nucleation mechanism of thin-film development has been divided into three main types. It depends on the interaction between the deposited atoms of the target and the substrate surface [22]. The metal creates the nanostructure form since the thickness (< ~30 nm) is not thick sufficient to make a continuous film [23]. Therefore, to modeling the ~10 nm Ag thin layer in the D/M/D structure, oblate nanoparticles with a relatively large distribution in their size can be used. For this, the half elliptical nanoparticles were utilized from a somewhat random combination of size, position, and angle to each other. The average size of elliptical Ag particles and their standard deviation (estimated close to experimental one[24]) are given in Table 1. This procedure of modeling was performed in the form of three samples with three different surface coverages (SCs) or SC1, SC2, and SC3 (Figure 4). These SCs of samples were selected qualitatively so that due to the lateral contact of particles with each other, they can characterize samples in the form of very high surface resistance (SR), acceptable SR, and very low SR, respectively. On the other hand, the metal nanostructure in these samples consists of particles separated from each other (SC1), somewhat separated from each other (SC2), and finally, the nanoparticles stick entirely to each other (SC3). These XY cross-sections are shown in Figure 4 (Figure 1-5 refers to the location of these cross-sections in the structure). For far-field (like reflection, transition, and absorption), the results were presented after averaging on the data of ten simulations. In these ten simulations for each case, the random distribution of nanostructure was different from each other, but the mean values determining the distribution characteristic of metallic nanostructure remained the same**.** The near-field results are comparative and are based on the specular maximum amount of field-intensity (E^2max) recorded in a typical vertical-plane section with the same geometric details for all samples.

Table 1. Ag nanostructures are modeled by a combination of half-elliptical particles. The particles size distribution (the average and its deviation along different axes)

X-Average (nm)	X-standard deviation (nm)	Y-Average (nm)	Y-standard deviation (nm)	Z-Average (Height) (nm)	Z-standard deviation (nm)
35	10	36	8	18	5

3. Result And Discussion

The interaction of light with D/M/D for three samples (SC1, Sc2, and Sc3) in the form of reflection, absorption, and transmission curves are shown in Figure 5. In the first comparison between Figures 3 and 5, the difference between the conventional D/M/D design and the nano-viewpoint is quite apparent. In the TMM method, due to the assumption of a homogeneous and uniform layer (10 nm) and according to the Beer-Lambert rule, the absorption is relatively small. However, due to the nanostructure of the Ag layer in D/M/D, the plasmonic resonance absorption losses are more essential. Plasmonic resonances are a function of the shape-size of the nanoparticles, the material of nanoparticles and the surrounding medium, and the form they are placed close to each other. Thus, contrary to Mie theory [25], which is commonly used for single spherical or near-spherical nanoparticles, 3D FDTD simulation is one of the main steps for the plasmonic study of these kinds of nanostructures. The simulation results show that this distribution of Ag nanoparticles in the D/M/D structure leads to a wide range of plasmonic resonance wavelengths from 400 nm.

In simple regard to D/M/D design (SC1, SC2, and SC3), it may seem that an appropriate strategy would be consisting of nanoparticles that, while interconnected, still have enough empty space (pinholes). In other words, the connected nanoparticles ensure reduced sheet resistance and enough open space provides proper light transmission. This form is well modeled in the SC2 sample. Nevertheless, what is observed by the simulated results is that plasmonic losses in this structure are significant and appropriate transparency cannot be attributed to it.

It may then appear that the use of a metal whose plasmonic wavelengths are not within this range, can reduce these plasmonic losses. Therefore, Al which shows its bulk plasmonics in the ultraviolet region may seem like a good alternative (instead of Ag) in the SC2 sample. The simulated absorption spectra for the three samples (SC1, SC2, and SC3 – metallic layer Ag or Al) are shown in Figure 6. The simulated results show that the nanostructured plasmonic peaks tend to red-shift in both cases. This means that for Ag, the plasmonic peaks of nanostructure are seen more in the range of 600 nm to 800 nm. But about Al, these peaks have been moved to the beginning of the visible area instead of UV. This behavior of Al can also harm the application of D/M/D, as a transparent layer. The imaginary part of the refractive index is directly related to losses inside the metal. The imaginary index value for Al is significantly higher than Ag. In contrast, the effects of plasmonic resonance loss for Ag can be significant. For showing this, a typical X-Z cross-section was selected for monitoring the near-field. The maximum amount of field intensity (E^2max) on this surface was recorded at each wavelength. This quantity is a function of the details of nanostructured D/M/D and can be used to compare near field effects between different modeled samples (Figure 7). The results of Figure 7 show that the near-field effect of Ag is more substantial than

those of Al. Therefore, according to Figures 6 and 7, Al doesn't offer a significant advantage over Ag in the D/M/D structure.

In this modeling, the SC3 sample compared to others is more similar to the TMM model. On the other hand, the SC3 represents the nanostructure with the least porosity, shows absorption behavior that can be partly explained by the coherence interference and the Beer-Lambert relationship. The decrease in the absorption behavior, especially compared to the SC2 sample, can confirm that the plasmonic effects are attenuated by the orientation of the nanostructure towards the continuous layer. In contrast, the SC1 sample, which describes a state with wholly separated particles, shows broad plasmonic peaks that are somewhat similar to the extinction curve of a single-particle with medium size. In SC2 which is more similar to the mean of these two later samples, the absorption is relatively high, especially from 500 nm onwards. This behavior may be related to the presence of the near-field coupling effect, in addition to the loss of plasmonic resonances associated with the nanostructure themselves[26].

Lastly, to add another aspect to the nano viewpoint in D/M/D design, the optical effect of Ag nanostructure on the surface roughness of the second layer was modeled (this part of the simulation was performed for SC2 sample, i.e., SC2-Rough). The presence of metallic nanostructure on the top surface of the first layer and during depositing the second layer may lead to an increase in the surface roughness of the second layer[27]. Figure 8 shows this model for the SC2 sample considering surface roughness. In this section of the modeling, roughness with dimensions commensurate with the metal Ag nanoparticles and aligned to them have been added to the surface of the second dielectric layer (In2O3). The curves of the optical response of SC2 and SC2-Rough samples are also shown in Figure 9. As can be seen, the addition of roughness to the model has not made a considerable change in far and near-field effect.

4. Conclusion

Paying attention to the nanostructural properties of D/M/D as a TCF during design has particular importance. In most thin-film fabrication methods, a continuous metallic layer with 10 nm thickness is not formed. Pre-fabrication designs are usually based on the 1D photonic crystal that this selected model does not conform to the experimental fabrication characteristics. In this research, 3D-FDTD modeling was performed based on the nanotechnology viewpoint of the metallic layer. Due to metal nanostructure, complex plasmonic behaviors occur that cannot be investigated by conventional theories. Therefore, three metal nanostructures that can represent cases with high (SC1), suitable (SC2), and low (SC3) sheet resistance were modeled for the simulation. SC2 sample refers to a metal nanostructure, where the particles have acceptable continuity (low surface resistance) and at the same time should be optically suitable due to the presence of sufficient light passage. The simulation results show that all three samples, especially sample SC2, have less optical transmission due to complex resonant plasmonic losses. This negative plasmonic effect is also effective for metals such as Al, even in the visible range. As an idea for proper designing, the simulation results emphasize that the fabrication methods should be engineered so that the particles are wholly adhered to and with a minimum height to form a metal nanostructure. In other words, with the relative approach of the metallic layer to the uniform one, we

reduce the complexity and diversity of plasmonic peaks to bulk plasmonic. Of course, in this case, it is better to pay attention to surface plasmonic polariton (SPP) as well. The effect of a rough surface in the second layer was modeled because of the presence of metal nanoparticles at the interface of the two layers. This roughness did not cause much change in near and far-field results.

Declarations

Acknowledgment

Thanks to Shahrekord University's rapid computing center for providing the simulations.

Funding

Not applicable

Conflicts of interest/Competing interests

The author declares no conflicts of interest.

Availability of data and material

Due to the increased size of the file after each simulation (usually about 50 GB or more), their storage is faced with hardware limitations.

Code availability

The Lumerical simulator is used for FDTD simulation.

Authors' contributions

Not applicable

Ethical approval

Not applicable

Consent to participate

Not applicable

Consent for publication

Not applicable

References

1. Ginley, D.S., H. Hosono, and D.C. Paine, *Handbook of Transparent Conductors*. 2010: Springer US.
2. Levy, D. and E. Castellón, *Transparent Conductive Materials: Materials, Synthesis, Characterization, Applications*. 2019: Wiley.
3. Jakšić, Z., *Micro and Nanophotonics for Semiconductor Infrared Detectors: Towards an Ultimate Uncooled Device*. 2014: Springer International Publishing.
4. Zhao, W., *Flexible Transparent Electrically Conductive Polymer Films for Future Electronics*. 2011: University of Akron.
5. Chen, Z., et al., *Fabrication of Highly Transparent and Conductive Indium–Tin Oxide Thin Films with a High Figure of Merit via Solution Processing.* Langmuir, 2013. **29**(45): p. 13836-13842.
6. Walker, A., et al., *Unconventional Thin Film Photovoltaics: RSC Energy and Environment Series*. 2016: Royal Society of Chemistry.
7. Cattin, L., J.C. Bernède, and M. Morsli, *Toward indium-free optoelectronic devices: Dielectric/metal/dielectric alternative transparent conductive electrode in organic photovoltaic cells.* physica status solidi (a), 2013. **210**(6): p. 1047-1061.
8. Akdemir, O., et al., *MoOx/Ag/MoOx multilayers as hole transport transparent conductive electrodes for n-type crystalline silicon solar cells.* International Journal of Energy Research, 2020. **44**(4): p. 3098-3109.
9. Fortunato, E., P. Barquinha, and L. Pereira, *Transparent Electronics*. Wiley.
10. Gould, R.D., S. Kasap, and A.K. Ray, *Thin Films*, in *Springer Handbook of Electronic and Photonic Materials*, S. Kasap and P. Capper, Editors. 2017, Springer International Publishing: Cham. p. 1-1.
11. Katsidis, C.C. and D.I. Siapkas, - *General transfer-matrix method for optical multilayer systems with coherent, partially coherent, and incoherent interference.* 2002.
12. Yang, J., et al., *Numerical and experimental investigation of highly flexible, transparent, and conductive WO3/Ag/PEI/CuSCN multilayered electrodes.* Optical Materials Express, 2020. **10**(12): p. 3257-3267.
13. Cattin, L., et al., *On the contribution of fullerene to the current of planar heterojunction organic solar cells.* Journal of Physics D: Applied Physics, 2020. **53**(22): p. 225501.
14. Kim, S. and J.-L. Lee, *Design of dielectric/metal/dielectric transparent electrodes for flexible electronics.* Journal of Photonics for Energy, 2012. **2**(1): p. 021215.
15. Ohring, M. and Knovel, *Materials Science of Thin Films*. 2002: Elsevier Science.
16. Baburin, A.S., et al., *Silver-based plasmonics: golden material platform and application challenges [Invited].* Optical Materials Express, 2019. **9**(2): p. 611-642.
17. Musa, S.M., *Computational Nanotechnology Using Finite Difference Time Domain*. 2017: CRC Press.
18. Nguyen, D.T., et al., *Effect of the thickness of the MoO3 layers on optical properties of MoO3/Ag/MoO3 multilayer structures.* Journal of Applied Physics, 2012. **112**(6): p. 063505.
19. Lim, S.-H. and H.-K. Kim, *Deposition Rate Effect on Optical and Electrical Properties of Thermally Evaporated WO3−x/Ag/WO3−x Multilayer Electrode for Transparent and Flexible Thin Film Heaters.*

Scientific Reports, 2020. **10**(1): p. 8357.
20. Malik, O., *Sputtered Indium Tin Oxide Films for Optoelectronic Applications*. 2017: IntechOpen.
21. Venkatachalam, S., *Optoelectronic Properties of ZnSe, ITO, TiO2 and ZnO Thin Films*. 2011: IntechOpen.
22. Rockett, A., *THIN FILM GROWTH PROCESSES*, in *The Materials Science of Semiconductors*. 2007, Springer US.
23. Martin, J. and J. Plain, *Fabrication of aluminium nanostructures for plasmonics.* Journal of Physics D: Applied Physics, 2014. **48**(18): p. 184002.
24. Ji, C., et al., *Ultrathin-metal-film-based transparent electrodes with relative transmittance surpassing 100%.* Nature Communications, 2020. **11**(1): p. 3367.
25. Hergert, W. and T. Wriedt, *The Mie Theory: Basics and Applications*. 2012: Springer Berlin Heidelberg.
26. Huang, Q., et al., *Graphene–Gold–Au@Ag NPs-PDMS Films Coated Fiber Optic for Refractive Index and Temperature Sensing.* IEEE Photonics Technology Letters, 2019. **31**(15): p. 1205-1208.
27. Ye, Y., et al., *Plasmonics of Diffused Silver Nanoparticles in Silver/Nitride Optical Thin Films.* Scientific Reports, 2019. **9**(1): p. 20227.

Figures

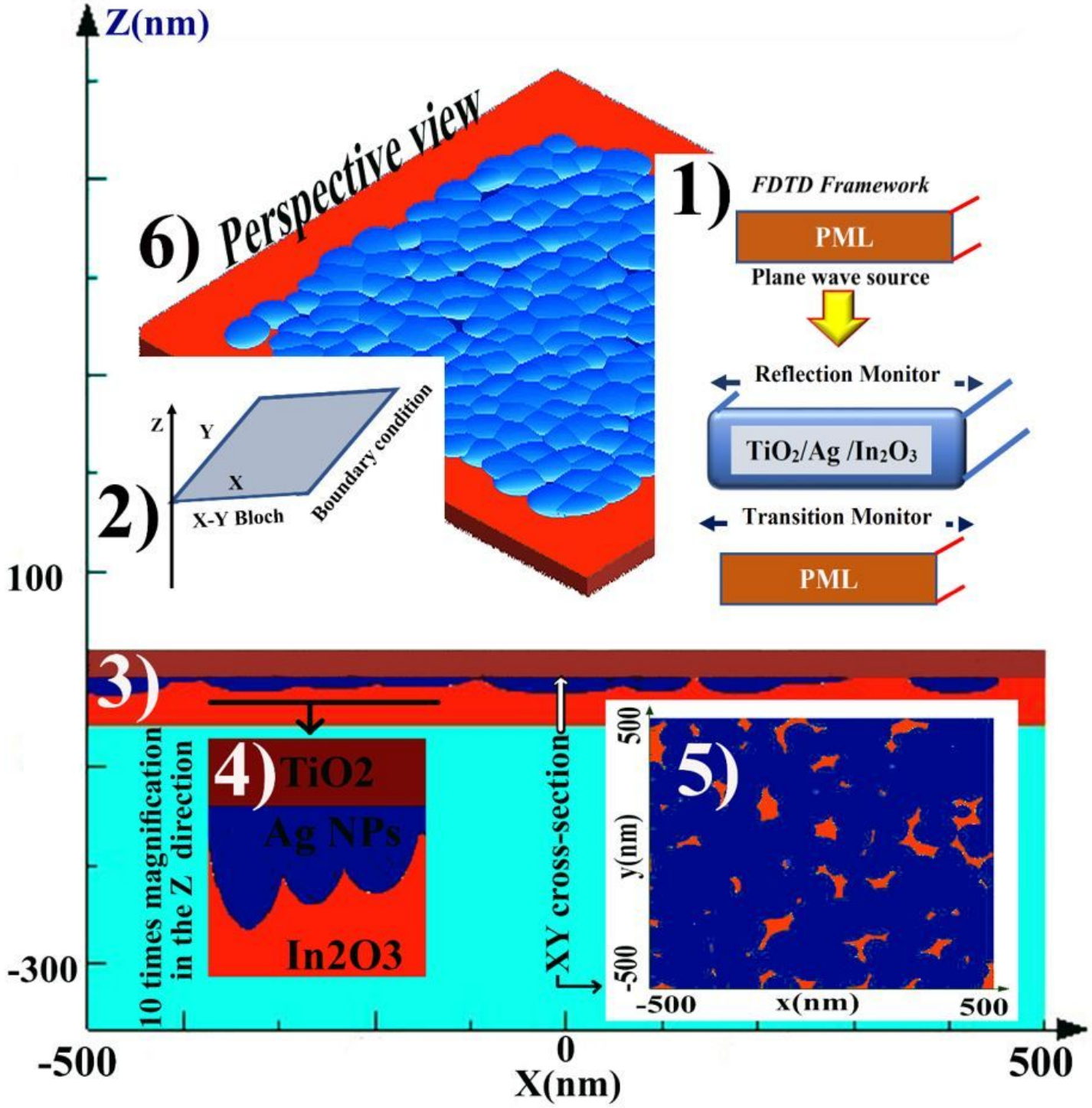

Figure 1

(1-6). Showing different aspects of the simulation. (1.1). 1D photonic crystal for FDTD simulation. PML boundary condition (BC) and plane wave source in the Z direction and periodic BC on the XY surface, (1.2). Demonstration of axes and Bloch BC for nanostructured simulation, (1.3) demonstration of nanostructured modeling of D/M/D, (1.4) Showing part of nanostructured modeling with magnification,

(1.5) Displays the porosity of a typical cross-section, (1.6) Typical 3D display of Ag nanostructure on the first dielectric layer of D/M/D.

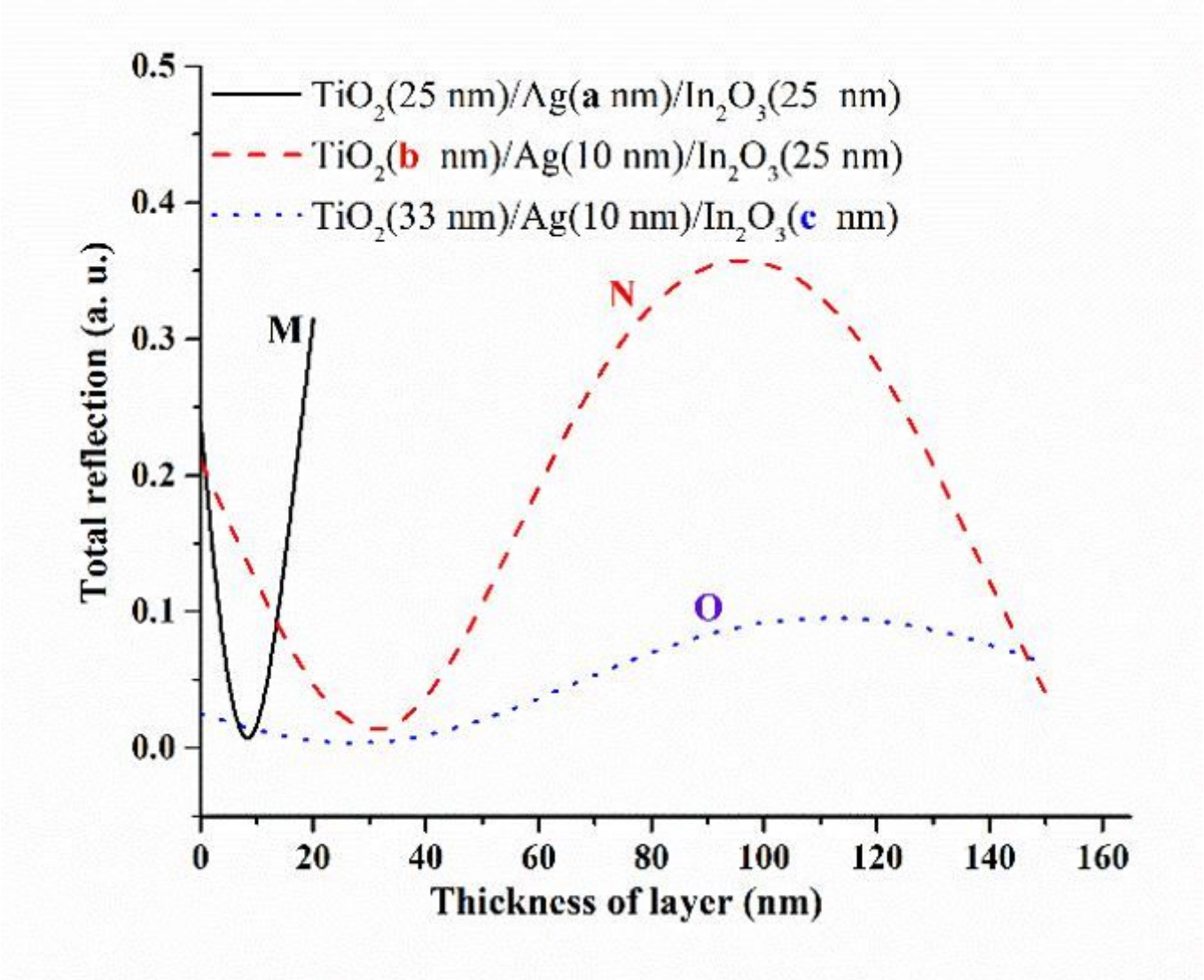

Figure 2

Showing reflection curves during design D/M/D based on 1D photonic crystal approach (by FDTD calculation). Curves M, N, and O are related to the change in thickness of Ag, TiO2, and In2O3, respectively.

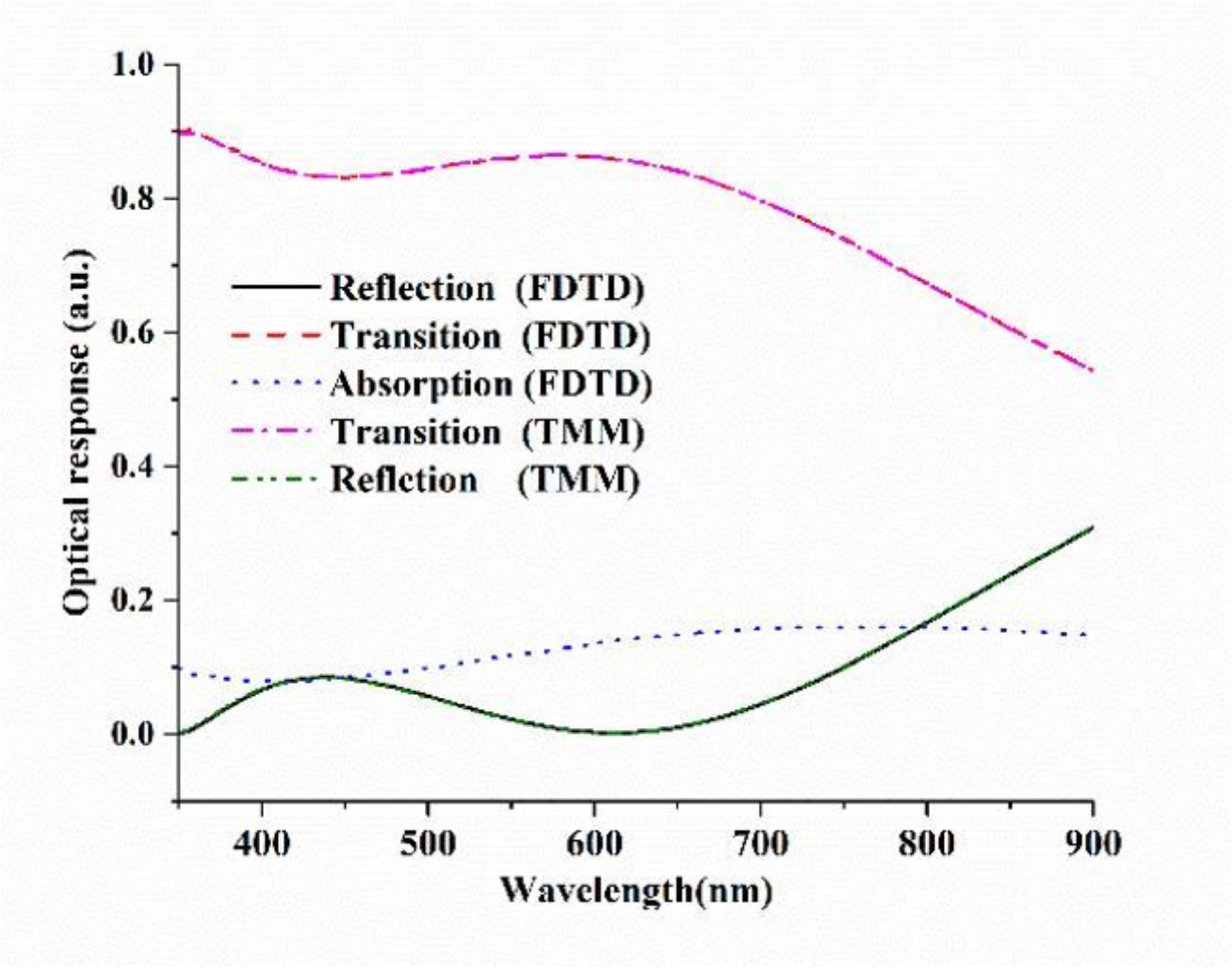

Figure 3

Far-field responses of 1D photonic crystal model of D/M/D, simulated by TMM and FDTD method (for this approach, the results of two methods are in good agreement).

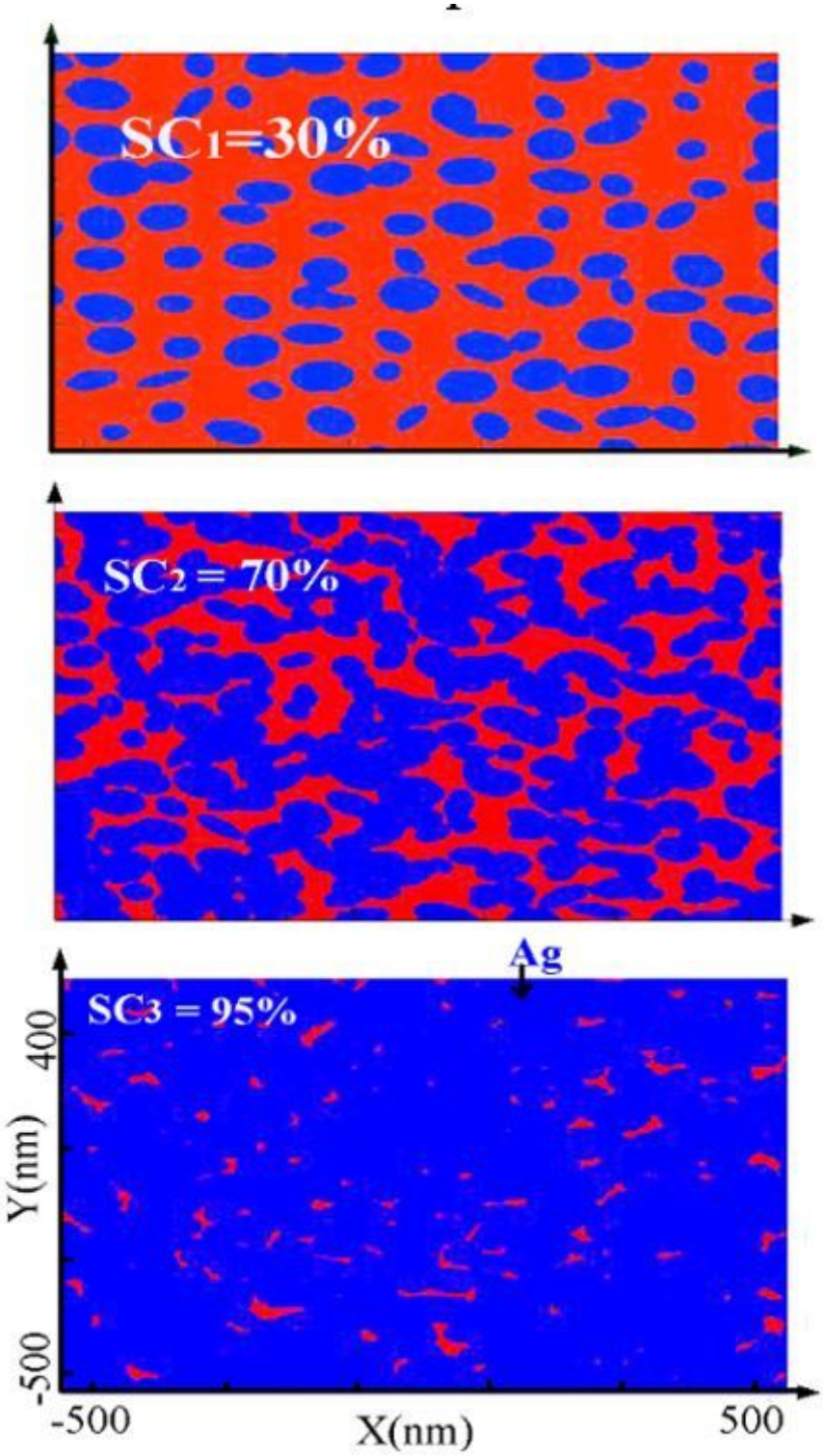

Figure 4

Cross-sections related to the three samples used in modeling. These samples were used to introduce three limit cases (i.e., style with high, acceptable, and very low sheet resistance).

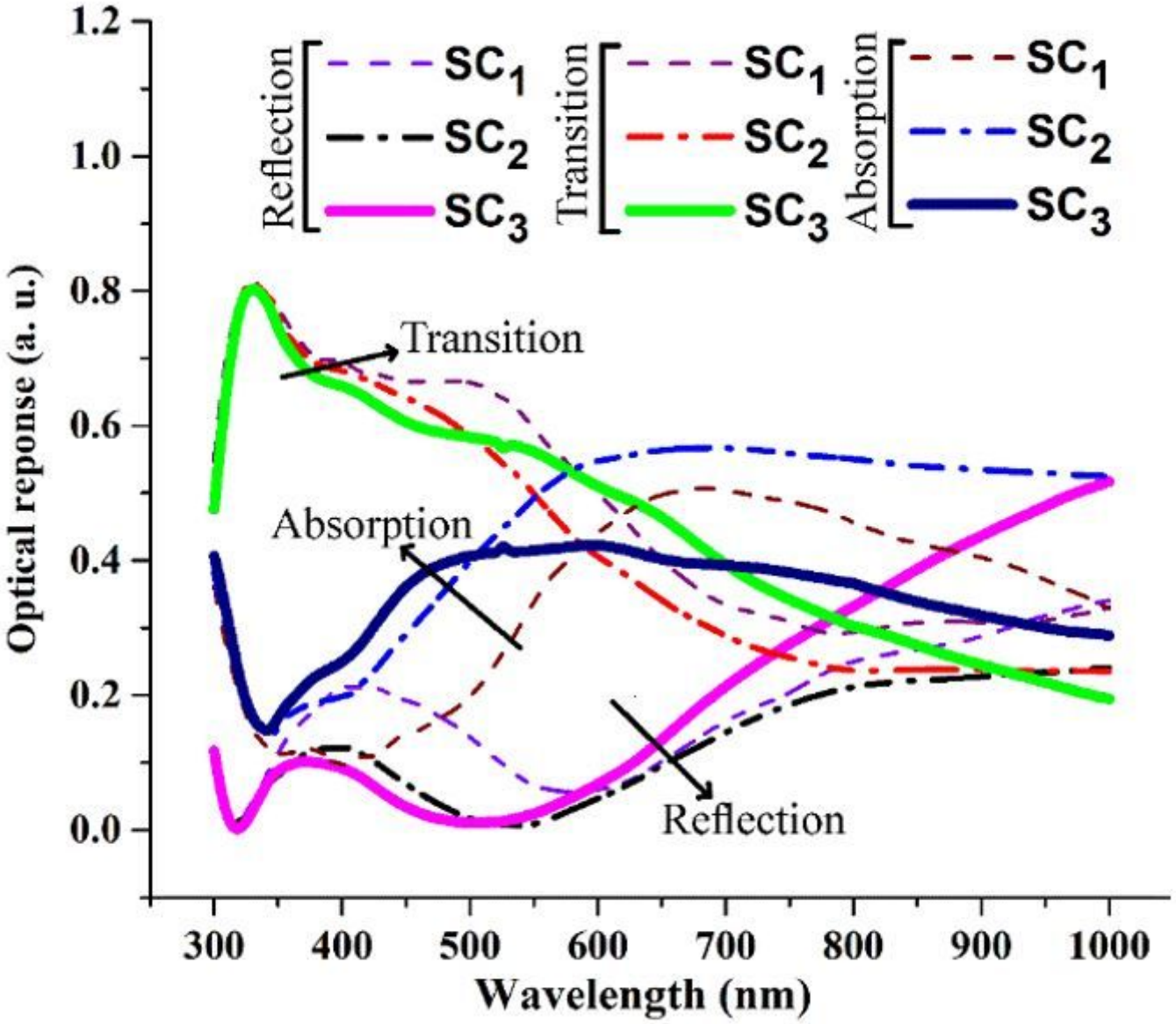

Figure 5

Far-field responses of the nanostructured model of D/M/D, simulated by FDTD method. The results were compared for three different modes SC1, SC2, and SC3.

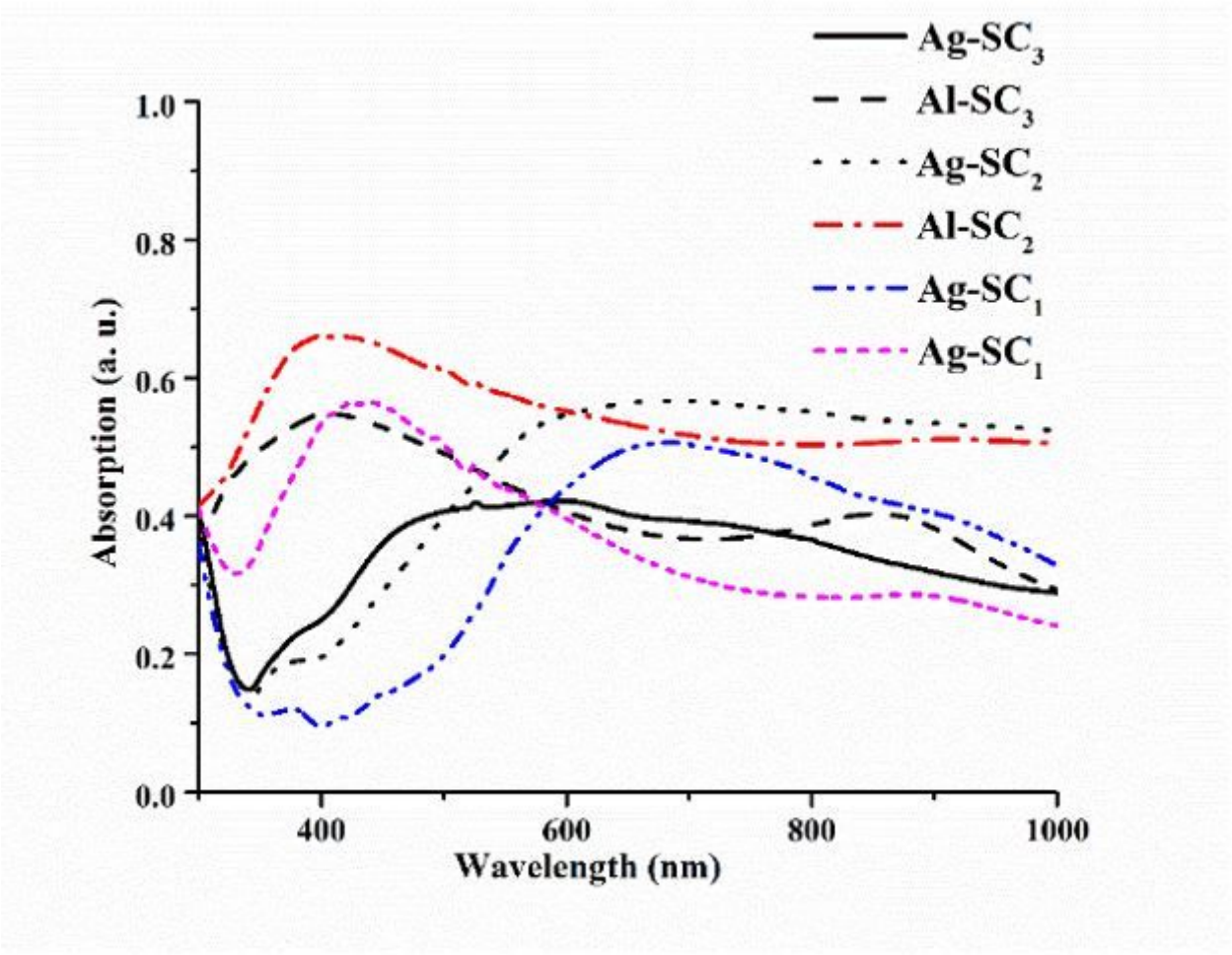

Figure 6

Absorption curves of models SC1, SC2, and SC3 for the case in which the material Ag and Al are selected for TiO2/M/In2O3.

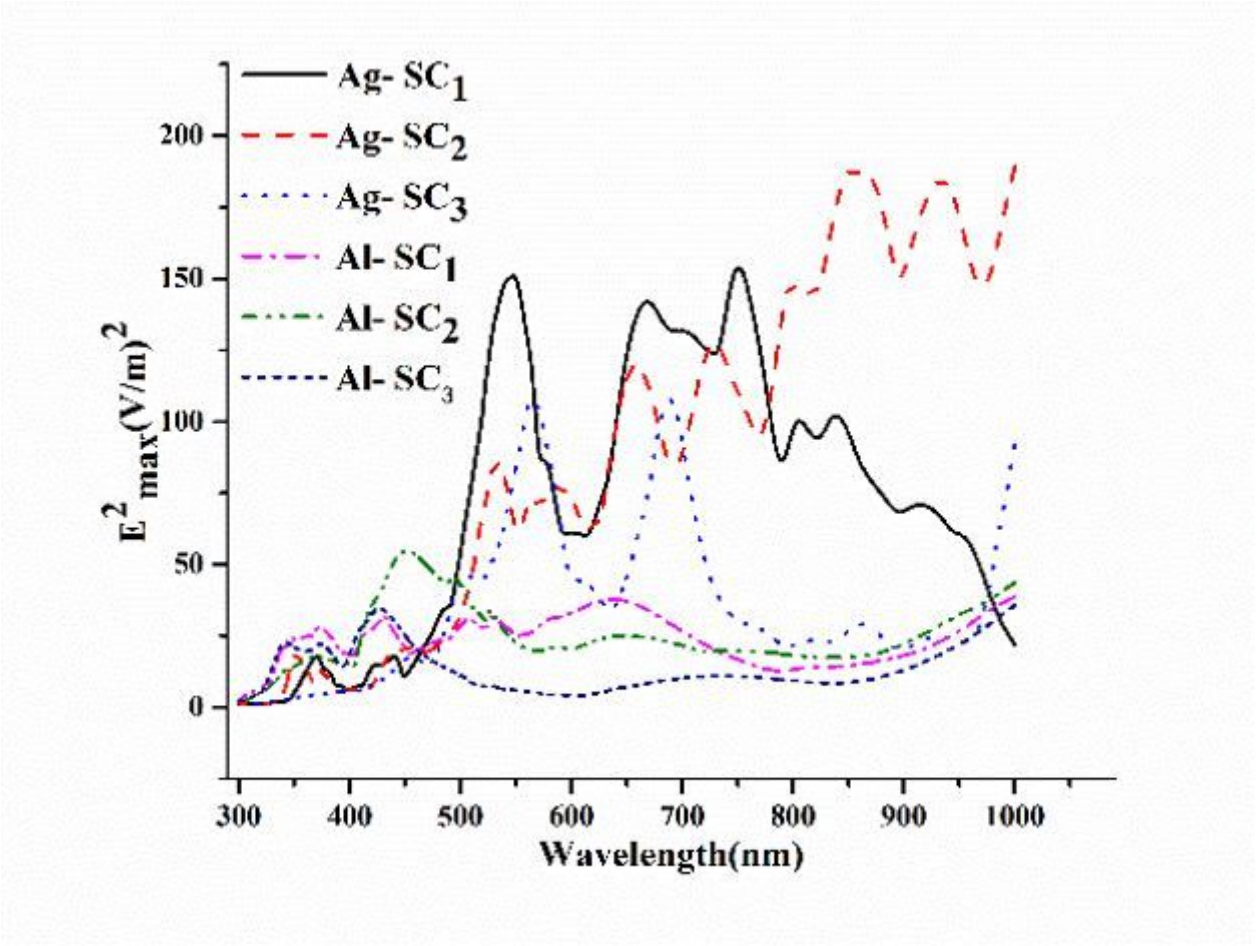

Figure 7

The maximum field intensity simulated at each wavelength on the selected typical cross-section for the three samples and different materials Ag and Al.

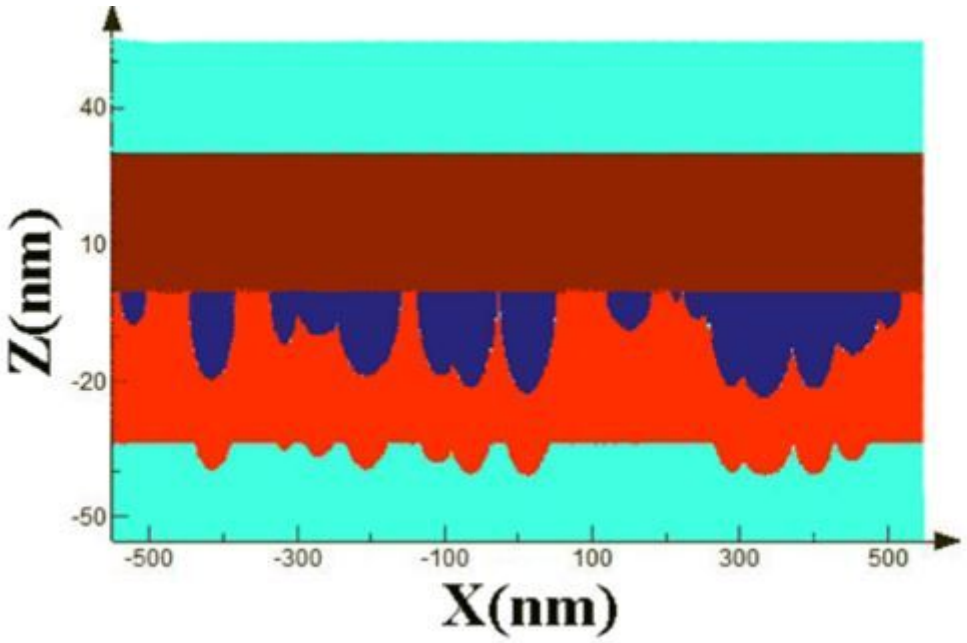

Figure 8

A representation of a typical vertical surface of 3D nanostructured D/M/D based on the SC2 Model, which a typical surface-roughness has also added to the surface of the second dielectric layer.

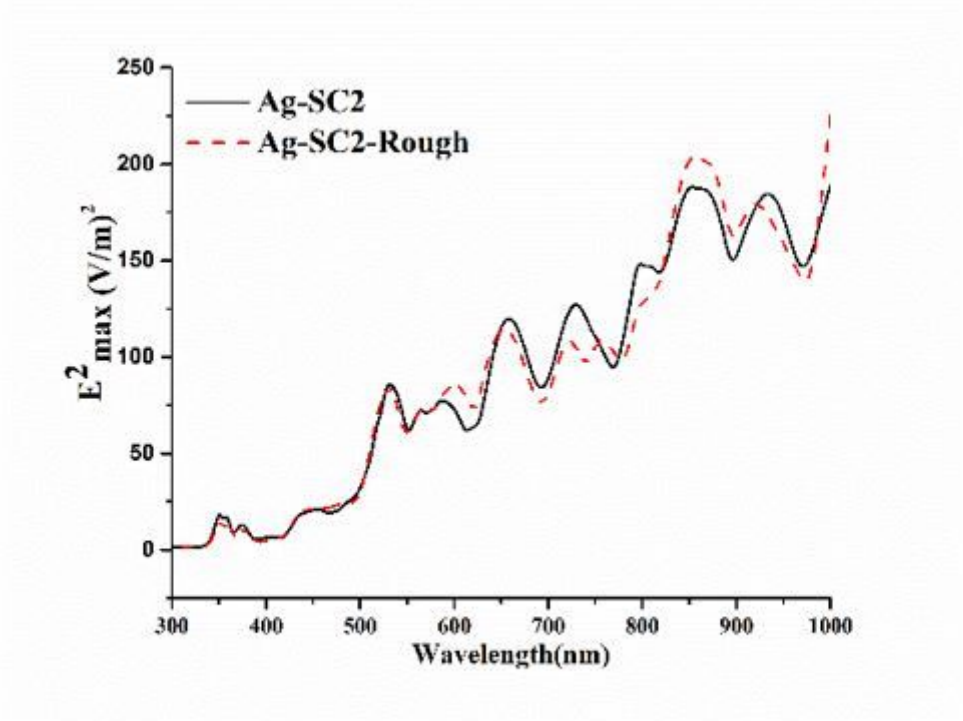

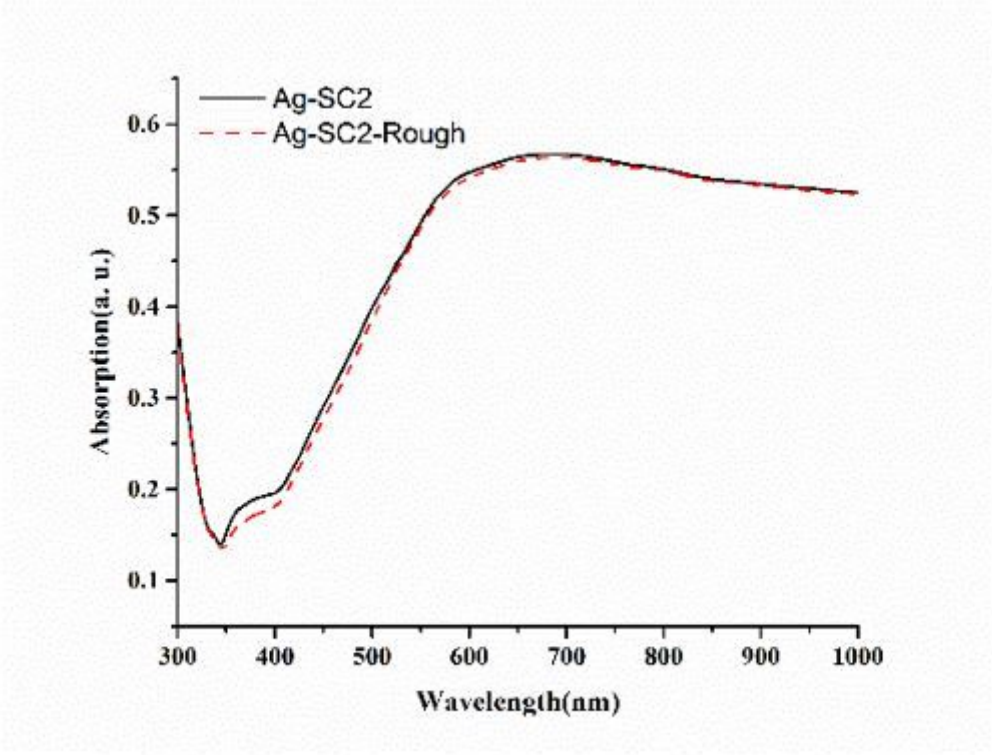

Figure 9

Display of maximum field intensity and absorption curve for two models Ag-SC2 and Ag-SC2-Rough.